Contribution from the Materials and Molecular Research Division, Lawrence Berkeley Laboratory and Department of Chemistry, University of California, Berkeley, California 94720

Syntheses and Crystal Structures of Tetrakis(diphenylamido)uranium(IV) and Bis(μ-oxo-tris(diphenylamido)uranium(IV)lithium diethyl etherate)

JOHN G. REYNOLDS, ALLAN ZALKIN,* DAVID H. TEMPLETON,* and NORMAN M. EDELSTEIN*

Received November 19, 1976 AIC60829W

The synthesis, crystal structure, optical and proton magnetic resonance spectra in solutions, and temperature-dependent magnetic susceptibility of the solid are reported for $U[(C_6H_5)_2N]_4$. The crystals are triclinic, of space group $P\bar{1}$; at 23 °C a = 10.74 (1) Å, b = 20.11 (2) Å, c = 9.86 (1) Å, α = 92.8 (1)°, β = 111.0 (1)°, γ = 99.4 (1)°, d_c = 1.55 g cm^{-3} for Z = 2. For 1372 reflections with $F^2 > 3\sigma$, R = 0.050 and R_w = 0.049. This compound is novel in exhibiting four-coordinate uranium(IV) in the crystalline state. The uranium atom is enclosed by a severely distorted tetrahedron of nitrogen atoms at distances 2.21 (2), 2.25 (2), 2.27 (2), and 2.35 (2) Å. A reaction product with air, $[UO[(C_6H_5)_2N]_3Li{\cdot}O(C_2H_5)_2]_2$, characterized by determination of its crystal structure, is orthorhombic, of space group *Pbca*; at 23 °C a = 21.29 (2) Å, b = 20.38 (2) Å, c = 16.13 (2) Å, d_c = 1.59 g cm^{-3} for Z = 8. For 2666 reflections with $F^2 > 3\sigma$, R = 0.038 and R_w = 0.041. The uranium atom is five-coordinate with U–N distances 2.33 (1), 2.34 (1), and 2.44 (1) Å and bridging oxygen atoms at 2.16 (1) and 2.20 (1) Å. The three-coordinate lithium atom is bonded to the bridging oxygen atom at 1.93 (3) Å, to the ether oxygen atom at 1.93 (3) Å, and to a nitrogen atom at 2.20 (3) Å.

Uranium dialkylamides were first synthesized by Jones et al.[1] as part of the search for volatile uranium compounds during the Manhattan Project. After the initial report 18 years elapsed before Bagnall and Yanir[2] reported the synthesis of uranium carbamates employing the uranium dialkylamides as intermediates. At approximately the same time, Jamerson and Takats[3] reported the synthesis of $(\eta\text{-}C_5H_5)_2U[N(C_2H_5)_2]_2$ again using $U[N(C_2H_5)_2]_4$ as an in situ intermediate in the reaction. We have recently reported the crystal structure and magnetic and optical properties of $U[N(C_2H_5)_2]_4$,[4] a dimer in the solid state, and of $U_3(CH_3NCH_2CH_2NCH_3)_6$,[5] a trimeric complex of U(IV). The latter compound was synthesized by the aminolysis reaction

$$M(NR_2)_4 + yHNR'_2 \rightarrow M(NR'_2)_y(NR_2)_{(4-y)} + yHNR_2 \quad (1)$$

instead of the more usual type of reaction

$$UCl_4 + 4LiNR_2 \rightarrow U(NR_2)_4 + 4LiCl \quad (2)$$

In order to prepare a monomeric uranium dialkylamide we have used R = C_6H_5 to hinder the oligomerization of $U(NR_2)_4$. We report the synthesis by both reactions 1 and 2,[6] the crystal structure, and the optical and magnetic properties of the monomeric complex $U(dpa)_4$ (dpa = $N(C_6H_5)_2$). In addition we report the crystal structure of $[UO(dpa)_3LiOEt_2]_2$, an oxygen-bridged reaction product of $U(dpa)_4$.

Experimental Section

Solvents. All solvents were dried and deoxygenated by refluxing with sodium and benzophenone under purified argon.

Reagents and Syntheses. All reactions and manipulations were done in a purified argon atmosphere or under vacuum. Diphenylamine was purchased from Aldrich and sublimed at 75 °C (10^{-4} mm) before use. *n*-Butyllithium and $LiNEt_2$ were purchased from Alfa-Ventron Corp. and used as received. UCl_4 was purchased from ROC/RIC Corp. and used as received.

$LiN(C_6H_5)_2$. To 0.25 mol of *n*-butyllithium was added 0.25 mol of diphenylamine in a large excess of pentane at 0 °C. After 24 h the mixture was Schlenk filtered and the precipitate vacuum dried.

$U(NEt_2)_4$. Synthesized as described earlier.[4]

$U[N(C_6H_5)_2]_4$, by Transamination. $U(NEt_2)_4$ (3.05 g, 0.0058 mol) was placed in a 250-ml Schlenk flask with 3.93 g (0.0230 mol) of diphenylamine. A noticeable red color was visible on the surface of the amine immediately upon contact with the amide. The flask was evacuated and 150 ml of pentane were added at liquid N_2 temperature. The mixture was allowed to react for 24 h at room temperature, although after 6 h no additional change was observed. The microcrystals were Schlenk filtered and dried by vacuum evaporation.

$U[N(C_6H_5)_2]_4$, by UCl_4 and Li(dpa). UCl_4 (2.5 g, 0.0066 mol) was added to 4.6 g (0.0263 mol) of Li(dpa) in a 250-ml Schlenk flask. The flask was then evacuated and 150 ml of diethyl ether was added at 77 K. The reaction was allowed to warm to room temperature and react for 24 h. The resulting precipitate was then Schlenk filtered and washed with benzene to remove the solid $U[N(C_6H_5)_2]_4$. The solution was then vacuum evaporated giving large red crystals.

$\{UO[N(C_6H_5)_2]_3LiO(C_2H_5)_2\}_2$. The filtrate from above was placed in a 250-ml Schlenk flask with a vacuum stopcock. The 24/40 ground glass joints were greased with Dow Corning No. 970 high-vacuum silicone grease. The stoppered flask remained in the air for periods longer than a month, at which time orange crystals had grown.

Physical Measurements. The proton magnetic resonance (^{1}H NMR) spectra were obtained by dissolving $U(dpa)_4$ in toluene-d_8 and THF-d_8 to form concentrated solutions (greater than 1 M for toluene-d_8, saturated for THF-d_8). Measurements were made on a Varian T-60 spectrometer with TMS as an internal reference, a Varian NV-14 spectrometer with a variable temperature insert using either benzene or TMS as an internal lock, and a Varian 220 MHz spectrometer equipped with a Nicolet Fourier Transform system and a variable temperature insert. NV-14 variable temperature measurements were made by circulating dry N_2 through a liquid N_2 cooling trap, then passing the cooled gas through a Minimite Model 238 temperature control unit (the unit was equipped with a Minimite thermocouple having an accuracy of ±1.0 °C). The Varian 220 MHz spectrometer was temperature calibrated with a methanol standard.

The optical spectra were obtained on a Cary 17 spectrometer at room temperature. The benzene samples prepared were 0.02 M solutions. The samples of $U(dpa)_4$ in diethyl ether were saturated solutions because of low solubility. No spectra of $U(dpa)_4$ could be obtained in pentane due to the low solubility. Sample cells of 0.5 cm path length were used with a matching 0.5 cm solvent cell in the reference compartment.

Magnetic susceptibility measurements were obtained with a PAR Model 155 vibrating sample magnetometer employing a homogeneous magnetic field produced by a Varian Associates 12-in. electromagnet capable of a maximum field strength of 12.5 kG. The magnetometer was calibrated with $HgCo(CNS)_4$.[7] A variable temperature liquid helium system produced sample temperatures in the range 1.5–100 K. Temperatures were measured with a calibrated GaAs diode placed approximately 0.5 in. above the sample. The ~0.1-g samples were placed in calibrated Kel-F containers which were weighed on a Cahn electrobalance. The filled capsules were stored in Schlenk tubes under argon and were transferred to the susceptibility apparatus under flowing N_2.

Both $U(dpa)_4$ and $UO(dpa)_3LiOEt_2$ are extremely sensitive to the atmosphere. Crystals were individually selected in an argon atmosphere drybox and placed inside 0.2-mm quartz capillaries with a tungsten needle. The capillaries were temporarily sealed with vacuum stopcock silicone grease and fire sealed immediately on their removal from the box. Data was collected with a Picker FACS-I automated diffractometer equipped with a graphite monochromator and a molybdenum tube. The cell dimensions were obtained from 2θ measurements (both positive and negative) for high order $h00$, $0k0$, and $00l$ reflections for the $U(dpa)_4$ crystal and from the angular positions of three manually centered reflections for the lithium compound; in each case $K\alpha_1$ peaks were resolved. The space groups

Table I. Summary of Crystal Data and Intensity Collection

Compd	$U[(C_6H_5)_2N]_4$	$UO[(C_6H_5)_2N]_3LiO(C_2H_5)_2$
Formula wt	910.90	839.75
a, Å	10.74 (1)	21.29 (2)
b, Å	20.11 (2)	20.38 (2)
c, Å	9.86 (1)	16.13 (2)
α, deg	92.8 (1)	90.0
β, deg	111.0 (1)	90.0
γ, deg	99.4 (1)	90.0
V, Å^3	1949	7000
Z	2	8
Space group	$P\bar{1}$	*Pbca*
Density(calcd), g/cm^3	1.55	1.59
Crystal shape and size	Irregular shape ~0.1 mm in diameter	Irregular particle about 0.4 × 0.2 × 0.1 mm
Crystal vol, mm^3	<0.001	~0.008
Temp, °C	22-23	22-23
Radiation	Mo $K\alpha_1$ (λ 0.709 26 Å), monochromated from (002) face of mosaic graphite	
μ, cm^{-1}	40	45
Scan method	ω	θ-2θ
Scan speed, deg/min	1	2
Receiving aperture	6 mm wide × 6 mm high, 33 cm from crystal	
Scan range, deg	2	2
Background	10-s counts at beginning and end of scan	10 s counts at 0.5° before and after scan limits
2θ range, deg	3-40	3-45
No. of scans including standards	3234	8467
Unique data, total	2529	6196
Unique data, $I > 3\sigma$	1372	2666
No. of variables	218	194
$R(I>3\sigma)$[a]	0.050	0.038
R_w[b]	0.049	0.041
Goodness of fit	1.00	1.18

[a] $R = \Sigma||F_o| - |F_o||/\Sigma|F_o|$. [b] $R_w = [\Sigma w(|F_o| - |F_c|)^2/\Sigma w|F_o|^2]^{1/2}$.

and cell dimensions are given in Table I. Three standard reflections were measured after each 200th scan to monitor for crystal decay, instrumental stability, and crystal alignment. No systematic variations of the standards were observed for the $U(dpa)_4$ crystals; for the $UO(dpa)_3LiOEt_2$ crystal a decay of 5% was observed and then corrected. The data were processed, averaged, and given estimated standard deviations using formulas presented in the Supplementary Material.

The $U(dpa)_4$ crystal used for the intensity measurements was very small (<0.1 mm) but was multiple, such that the ω scans of a selected set of reflections showed two peaks separated by as low as 0.15° and as high as 0.50°; the two peaks were approximately equal in height and their half-widths were about 0.1°. Since a θ–2θ scan could not collect the integrated intensity an ω scan technique was used to collect the data. No absorption correction was made because of the difficulty of measuring the dimensions of the crystal and testing their validity. The factor $p = 0.05$ was used in the calculation of $\sigma(F^2)$.

The $UO(dpa)_3LiOEt_2$ crystal intensities were obtained by a θ–2θ scan. The half-width of the ω scan was about 0.13°, with a satellite shoulder of about one-third of the main peak; the whole integrated peak was obtainable in a θ–2θ scan technique. Intensities of several reflections, measured at various azimuthal angles, varied 8 to 21% between extreme values. The crystal was irregularly shaped with no clear facets, and the optical image as viewed through a microscope was severely distorted by the capillary. The dimensions of the crystal were estimated, and a set of planes to define its shape was selected. Because an absorption correction based on these measurements failed to account properly for the observed intensity variations no correction was applied. The factor $p = 0.03$ was used in the calculation of $\sigma(F^2)$.

For both compounds, the Patterson function revealed the positions of the uranium atoms, and the subsequent electron density Fourier using uranium phases gave the positions of all the non-hydrogen atoms. The structures were refined by full-matrix least squares where the function $\Sigma w(|F_o| - |F_c|)^2$ was minimized. No corrections for extinction were indicated, and none were made. Each hydrogen atom was included at its estimated position at a distance of 0.95 Å from its carbon atom and included in the calculations of the structure factor, but was not refined. The introduction of hydrogen atoms in the refinements caused shifts in some carbon–carbon bond distances more than their esd's, and reduced those in the phenyl rings an average of 0.03 Å in each crystal. Thus even when hydrogen atoms cannot be resolved

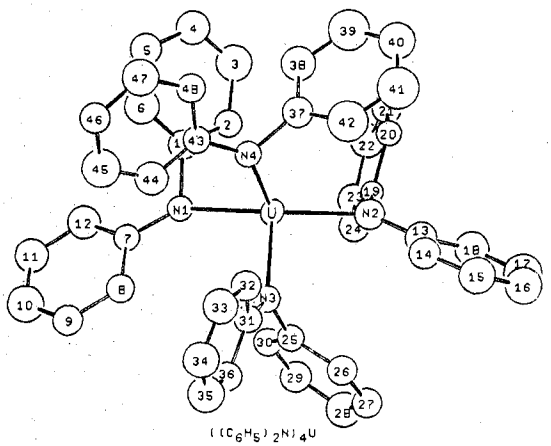

Figure 1. Molecular structure of $U[(C_6H_5)_2N]_4$.

their introduction gives a better description of the rest of the structure. The least-squares refinements converged well enough so that no parameter shifted more than 0.02σ for $U(dpa)_4$ or 0.11σ for the other structure.

The final difference Fourier maps showed no additional atoms. In the $U(dpa)_4$ structure the largest peak was 1.6 e/Å^3 and was about 1.06 Å from both N(4) and C(37) and represents background noise. For the $UO(dpa)_3LiOEt_2$ structure, the largest peak was 2 e/Å^3 and was 0.7 Å from the uranium atom; the second and third peaks were also close to uranium.

Final positional and thermal parameters are given in Tables II and III; the temperature factors have the form $\exp[-0.25(h^2a^{*2}B_{11} + ... + 2hka^*b^*B_{12} + ...)]$ for anisotropic atoms and $\exp(-B\lambda^{-2}\sin^2\theta)$ for isotropic atoms with the units of B in both cases being Å^2. The distances (uncorrected for thermal motion) and angles are listed in Tables IV through VII.

Discussion

$U(dpa)_4$ is a monomer in the solid state and exhibits a four-coordination which is novel for U(IV). A picture of the complex is shown in Figure 1, and a stereogram is shown in

Table II. Parameters for $U(dpa)_4$

Atom	x	y	z	B, Å²	Atom	x	y	z	B, Å²
U	0.259 8 (1)	0.244 14 (7)	0.157 2 (1)	*a*	C(43)	0.397 (3)	0.286 (1)	0.525 (3)	3.0 (7)
N(1)	0.482 (2)	0.290 (1)	0.179 (2)	2.6 (5)	C(44)	0.457 (3)	0.349 (2)	0.512 (3)	4.5 (7)
N(2)	0.079 (2)	0.165 (1)	0.011 (2)	3.7 (5)	C(45)	0.545 (3)	0.390 (1)	0.633 (4)	6.0 (8)
N(3)	0.164 (2)	0.336 (1)	0.115 (2)	2.9 (5)	C(46)	0.574 (3)	0.370 (1)	0.773 (3)	3.7 (7)
N(4)	0.303 (2)	0.247 (1)	0.395 (2)	2.7 (5)	C(47)	0.518 (3)	0.304 (2)	0.781 (3)	5.5 (8)
C(1)	0.541 (3)	0.231 (1)	0.245 (3)	3.5 (7)	C(48)	0.428 (3)	0.263 (1)	0.662 (3)	3.4 (7)
C(2)	0.493 (2)	0.166 (1)	0.165 (3)	3.0 (6)	H(1)	0.427	0.1598	0.0681	6.000
C(3)	0.542 (3)	0.109 (1)	0.227 (3)	5.4 (8)	H(2)	0.5089	0.0644	0.1745	6.000
C(4)	0.637 (3)	0.121 (1)	0.363 (3)	4.6 (7)	H(3)	0.6710	0.0833	0.4094	6.000
C(5)	0.689 (3)	0.186 (1)	0.439 (3)	3.9 (7)	H(4)	0.7619	0.192	0.5312	6.000
C(6)	0.638 (3)	0.241 (1)	0.384 (3)	4.9 (8)	H(5)	0.6696	0.284	0.4398	6.000
C(7)	0.567 (3)	0.351 (1)	0.187 (3)	2.7 (6)	H(6)	0.4219	0.4083	0.1723	6.000
C(8)	0.513 (3)	0.410 (1)	0.178 (3)	3.2 (7)	H(7)	0.5632	0.5123	0.1747	6.000
C(9)	0.597 (3)	0.471 (1)	0.176 (3)	3.7 (7)	H(8)	0.7765	0.5151	0.1721	6.000
C(10)	0.724 (3)	0.473 (2)	0.177 (3)	5.5 (8)	H(9)	0.8666	0.418	0.1864	6.000
C(11)	0.777 (3)	0.416 (2)	0.184 (3)	4.6 (7)	H(10)	0.7297	0.3129	0.1877	6.000
C(12)	0.695 (3)	0.354 (1)	0.186 (3)	4.4 (7)	H(11)	−0.0728	0.2223	0.1275	6.000
C(13)	−0.063 (3)	0.156 (1)	−0.034 (3)	4.1 (8)	H(12)	−0.3087	0.2013	0.0505	6.000
C(14)	−0.127 (3)	0.191 (1)	0.043 (3)	4.0 (7)	H(13)	−0.442	0.1344	−0.1572	6.000
C(15)	−0.268 (3)	0.180 (1)	−0.006 (3)	5.4 (8)	H(14)	−0.3499	0.0782	−0.2953	6.000
C(16)	−0.346 (3)	0.140 (2)	−0.127 (3)	5.6 (8)	H(15)	−0.1113	0.0888	−0.2200	6.000
C(17)	−0.291 (3)	0.106 (1)	−0.208 (3)	6.0 (8)	H(16)	0.1252	0.0464	0.0746	6.000
C(18)	−0.149 (3)	0.113 (1)	−0.165 (3)	4.8 (8)	H(17)	0.2327	−0.0231	−0.023	6.000
C(19)	0.134 (2)	0.122 (1)	−0.059 (3)	2.0 (6)	H(18)	0.3161	0.0112	−0.2032	6.000
C(20)	0.155 (2)	0.060 (1)	−0.002 (2)	2.6 (6)	H(19)	0.2643	0.1111	−0.3055	6.000
C(21)	0.220 (3)	0.019 (1)	−0.059 (3)	3.4 (7)	H(20)	0.1616	0.1830	−0.2137	6.000
C(22)	0.267 (3)	0.039 (1)	−0.168 (3)	4.7 (8)	H(21)	−0.090	0.3304	−0.0628	6.000
C(23)	0.238 (3)	0.099 (1)	−0.226 (3)	4.0 (7)	H(22)	−0.1724	0.3115	−0.3157	6.000
C(24)	0.177 (3)	0.141 (1)	−0.175 (3)	3.7 (7)	H(23)	−0.0303	0.3128	−0.4504	6.000
C(25)	0.112 (3)	0.333 (1)	−0.038 (3)	2.9 (6)	H(24)	0.1973	0.3168	−0.3196	6.000
C(26)	−0.030 (3)	0.327 (1)	−0.114 (3)	3.6 (7)	H(25)	0.2907	0.3348	−0.0654	6.000
C(27)	−0.077 (3)	0.317 (1)	−0.264 (3)	3.6 (7)	H(26)	0.1299	0.461	0.0546	6.000
C(28)	0.006 (3)	0.316 (1)	−0.347 (3)	5.0 (8)	H(27)	0.1414	0.3414	0.3727	6.000
C(29)	0.138 (3)	0.320 (1)	−0.268 (3)	3.9 (7)	H(28)	0.1449	0.4355	0.520	6.000
C(30)	0.195 (3)	0.330 (1)	−0.115 (3)	3.2 (7)	H(29)	0.1214	0.5381	0.4363	6.000
C(31)	0.146 (2)	0.388 (1)	0.197 (3)	3.1 (7)	H(30)	0.1113	0.5468	0.1992	6.000
C(32)	0.142 (3)	0.384 (1)	0.335 (3)	3.7 (7)	H(31)	0.3988	0.1315	0.4311	6.000
C(33)	0.138 (3)	0.441 (2)	0.422 (3)	5.0 (8)	H(32)	0.2795	0.0208	0.3983	6.000
C(34)	0.127 (3)	0.501 (2)	0.377 (3)	5.3 (8)	H(33)	0.0599	0	0.3895	6.000
C(35)	0.122 (3)	0.505 (1)	0.237 (3)	5.5 (8)	H(34)	−0.057	0.0891	0.3767	6.000
C(36)	0.132 (3)	0.453 (1)	0.150 (3)	3.5 (7)	H(35)	0.0613	0.1984	0.3988	6.000
C(37)	0.239 (3)	0.177 (1)	0.403 (3)	3.8 (7)	H(36)	0.4368	0.3642	0.418	6.000
C(38)	0.304 (3)	0.123 (2)	0.414 (3)	4.8 (8)	H(37)	0.5884	0.4338	0.6219	6.000
C(39)	0.235 (4)	0.058 (2)	0.401 (3)	6.9 (9)	H(38)	0.6268	0.4002	0.8593	6.000
C(40)	0.105 (3)	0.045 (2)	0.392 (3)	5.4 (8)	H(39)	0.5462	0.2857	0.8728	6.000
C(41)	0.036 (3)	0.097 (2)	0.387 (3)	7.3 (9)	H(40)	0.3850	0.2192	0.6715	6.000
C(42)	0.106 (4)	0.161 (2)	0.396 (3)	6.7 (9)					

[a] $B_{11} = 2.00\ (6); B_{22} = 2.80\ (6); B_{33} = 3.11\ (6); B_{12} = 0.49\ (4); B_{13} = 0.73\ (5); B_{23} = 0.35\ (4)$.

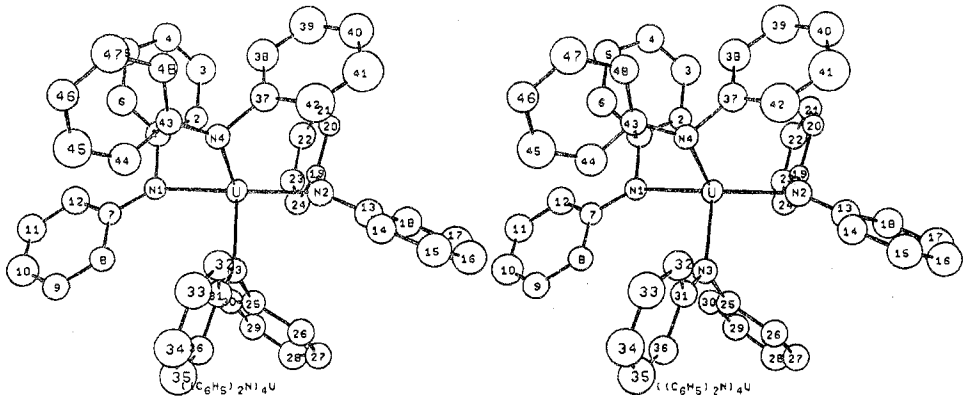

Figure 2. Stereogram of $U[(C_6H_5)_2N]_4$.

Figure 2. Although the uranium atom is coordinated to four nitrogen atoms, the calculated angles in Table V are far from those for a regular tetrahedron, or for any other regular geometrical figure. The U–N bond distances listed in Table IV vary from 2.21 through 2.35 Å and average 2.27 Å. This average value compares with single bond values of 2.22 Å in $[U(NEt_2)_4]_2$[4] and 2.21 Å in $U_3(CH_3NCH_2CH_2NCH_3)_6$.[5] As previously reported for transition metal amides,[8-13] the M–N–C_2 atoms form a plane for terminal amide groups. This planarity has been attributed to $p\pi \rightarrow d\pi$ bonding in the d transition series. We have found this fact very useful in distinguishing a three- from a four-coordinate amide nitrogen.

The nitrogen–carbon bond lengths are shorter for $U(dpa)_4$ than for other uranium alkylamides. The average value of 1.42

Table III. Parameters for $UO(dpa)_3Li{\cdot}O(C_2H_5)_2$

Atom	x	y	z	B, Å²	Atom	x	y	z	B, Å²
U	−0.003 95 (2)	0.020 35 (2)	0.105 48 (2)	*a*	C(39)	0.267 (1)	0.072 (1)	0.058 (2)	13.9 (8)
O(1)	−0.060 1 (3)	0.008 8 (4)	−0.005 2 (5)	2.9 (1)	C(40)	0.250 (1)	0.139 (1)	0.070 (1)	10.4 (6)
N(1)	−0.072 2 (4)	0.083 1 (5)	0.185 9 (6)	3.6 (2)	Li	0.130 (1)	0.050 (1)	0.024 (2)	5.2 (5)
N(2)	0.081 7 (4)	0.098 3 (5)	0.127 3 (6)	3.5 (2)	H(1)	−0.191 5	0.087 0	0.231 3	6.000
N(3)	−0.024 2 (4)	−0.084 2 (5)	0.159 1 (6)	3.6 (2)	H(2)	−0.274 2	0.143 2	0.164 8	6.000
C(1)	−0.123 3 (6)	0.118 8 (6)	0.151 4 (7)	3.8 (3)	H(3)	−0.254 8	0.208 5	0.055 3	6.000
C(2)	−0.183 6 (6)	0.113 2 (7)	0.183 7 (8)	4.8 (3)	H(4)	−0.155 4	0.217 6	−0.002 6	6.000
C(3)	−0.232 5 (6)	0.147 2 (7)	0.144 7 (9)	5.6 (3)	H(5)	−0.071 3	0.162 9	0.061 9	6.000
C(4)	−0.220 9 (6)	0.184 9 (7)	0.079 4 (9)	5.5 (3)	H(6)	−0.088 8	0.178 8	0.297 0	6.000
C(5)	−0.162 1 (7)	0.191 4 (7)	0.045 (1)	6.4 (4)	H(7)	−0.077 6	0.178 2	0.432 3	6.000
C(6)	−0.112 7 (6)	0.158 4 (7)	0.083 1 (9)	5.2 (3)	H(8)	−0.055 6	0.082 7	0.504 5	6.000
C(7)	−0.069 0 (5)	0.081 6 (6)	0.273 3 (8)	3.7 (3)	H(9)	−0.039 9	−0.013 8	0.429 9	6.000
C(8)	−0.078 1 (7)	0.138 8 (8)	0.323 (1)	5.9 (3)	H(10)	−0.053 5	−0.015 1	0.288 9	6.000
C(9)	−0.072 3 (7)	0.138 3 (8)	0.403 (1)	6.8 (4)	H(11)	0.026 7	0.150 8	0	6.000
C(10)	−0.058 9 (6)	0.082 4 (8)	0.446 (1)	5.6 (3)	H(12)	0.023 7	0.260 3	−0.042	6.000
C(11)	−0.050 5 (6)	0.025 6 (8)	0.401 8 (9)	5.9 (3)	H(13)	0.077 4	0.337 2	0.031 3	6.000
C(12)	−0.057 1 (5)	0.025 4 (7)	0.317 8 (8)	4.7 (3)	H(14)	0.141	0.311 1	0.141 0	6.000
C(13)	0.082 4 (5)	0.165 8 (6)	0.102 4 (8)	3.6 (2)	H(15)	0.139 7	0.203 1	0.189 5	6.000
C(14)	0.048 5 (7)	0.183 3 (7)	0.030 7 (9)	5.5 (3)	H(16)	0.125 9	−0.009 7	0.174	6.000
C(15)	0.047 3 (8)	0.248 (1)	0.005 (1)	7.6 (4)	H(17)	0.141 9	−0.051 4	0.307 5	6.000
C(16)	0.080 1 (9)	0.292 7 (9)	0.048 (1)	8.0 (5)	H(18)	0.126 4	0.019	0.421 0	6.000
C(17)	0.116 3 (8)	0.279 (1)	0.114 (1)	7.9 (4)	H(19)	0.087	0.120	0.402 6	6.000
C(18)	0.115 8 (7)	0.214 2 (9)	0.142 (1)	6.2 (4)	H(20)	0.067 6	0.162	0.273 7	6.000
C(19)	0.096 0 (6)	0.078 8 (6)	0.208 5 (8)	4.0 (3)	H(21)	−0.019 0	−0.138 6	0.308 2	6.000
C(20)	0.117 6 (6)	0.017 4 (8)	0.220 8 (8)	5.1 (3)	H(22)	0.062 5	−0.201 6	0.365 6	6.000
C(21)	0.128 0 (6)	−0.007 6 (7)	0.299 6 (9)	5.4 (3)	H(23)	0.151 6	−0.222	0.293 7	6.000
C(22)	0.117 5 (6)	0.033 9 (8)	0.366 4 (9)	5.3 (3)	H(24)	0.163 7	−0.183 3	0.161 8	6.000
C(23)	0.095 2 (6)	0.093 6 (7)	0.355 3 (9)	5.1 (3)	H(25)	0.080 9	−0.121 3	0.096	6.000
C(24)	0.083 6 (6)	0.118 8 (7)	0.279 7 (9)	4.8 (3)	H(26)	−0.127 5	−0.020 3	0.150 9	6.000
C(25)	0.022 6 (5)	−0.123 4 (6)	0.197 2 (7)	3.6 (2)	H(27)	−0.233 5	−0.056 4	0.152 1	6.000
C(26)	0.017 7 (6)	−0.147 3 (6)	0.276 5 (8)	4.8 (3)	H(28)	−251 2	−0.168 7	0.164 1	6.000
C(27)	0.066 9 (7)	−0.184 8 (7)	0.311 0 (9)	5.5 (3)	H(29)	−0.175 0	−0.240 9	0.173 6	6.000
C(28)	0.119 0 (6)	−0.197 1 (7)	0.268 8 (8)	4.9 (3)	H(30)	−0.068 4	−0.207	0.169 3	6.000
C(29)	0.125 9 (6)	−0.174 4 (7)	0.191 1 (9)	5.4 (3)	H(31)	0.271 0	−0.024 1	−0.016 9	12.000
C(30)	0.076 6 (6)	−0.136 6 (7)	0.151 4 (8)	4.8 (3)	H(32)	0.206 7	−0.056 8	0.001 6	12.000
C(31)	−0.086 1 (6)	−0.110 0 (7)	0.163 5 (8)	4.4 (3)	H(33)	0.237 4	−0.073 9	0.139 3	12.000
C(32)	−0.136 3 (7)	−0.065 8 (7)	0.156 1 (8)	5.5 (3)	H(34)	0.301 7	−0.041 2	0.120 8	12.000
C(33)	−0.199 6 (7)	−0.086 5 (8)	0.156 5 (9)	6.4 (4)	H(35)	0.284 9	−0.108	0.080 4	12.000
C(34)	−0.209 1 (8)	−0.153 3 (9)	0.163 (1)	7.0 (4)	H(36)	0.292 7	0.068 7	0.009 7	12.000
C(35)	−0.164 9 (9)	−0.195 8 (9)	0.169 (1)	8.0 (5)	H(37)	0.290 8	0.057 4	0.104 7	12.000
C(36)	−0.100 9 (7)	−0.175 2 (8)	0.167 5 (9)	5.7 (4)	H(38)	0.224 7	0.142 8	0.118 5	12.000
O(2)	0.214 6 (4)	0.031 2 (5)	0.048 5 (6)	5.8 (2)	H(39)	0.226 6	0.154	0.023 4	12.000
C(37)	0.239 4 (9)	−0.031 (1)	0.024 (1)	9.1 (5)	H(40)	0.286 5	0.165 2	0.076 3	12.000
C(38)	0.268 5 (9)	−0.067 (1)	0.098 (1)	10.2 (5)					

[a] $B_{11} = 2.32\ (2); B_{22} = 2.75\ (2); B_{33} = 2.43\ (1); B_{12} = -0.10\ (2); B_{13} = 0.00\ (2); B_{23} = -0.06\ (2)$.

Å corresponds to a nitrogen–sp^2 carbon single bond length.[14] In aromatic amines this shorter length can be attributed to the sp^2 character of the aromatic carbon and the delocalization of the nitrogen lone pair into the aromatic π system. The average U–N bond length is longer than that for the alkylamides. This could also be attributed to the delocalization effect where the lone pair is not as available for metal–ligand π bonding, as in the alkylamides. However, steric interactions cannot be ruled out. One U–N bond is significantly longer than the other three. A similar phenomenon is observed with certain niobium(V) alkylamides[10] where the one M–N bond is much *shorter*. This behavior has been attributed to steric crowding alone since the delocalization effect is not possible in these systems. The phenyl rings attached to the same nitrogen atom tend to be perpendicular to each other with dihedral angles of 70, 79, 81, and 90°, see Figure 2.

The uranium in $UO(dpa)_3LiOEt_2$ is five-coordinate and is dimerized via oxygen bridge bonds; the dimer is centered on a center of symmetry, see Figures 3 and 4. The U–U approach across the center is 3.50 Å, and the U–O bridge bonds are 2.16 and 2.20 Å. The uranium is at the center of an approximate trigonal bipyramid in which N(1) and O(1)′ are the apices and N(2), N(3), and O(1) are on the equator. This is similar to the coordination geometry described for uranium in $U(NEt_2)_4$. The U–N bond lengths in this compound (Table VI) also are longer than the single U–N bond lengths in

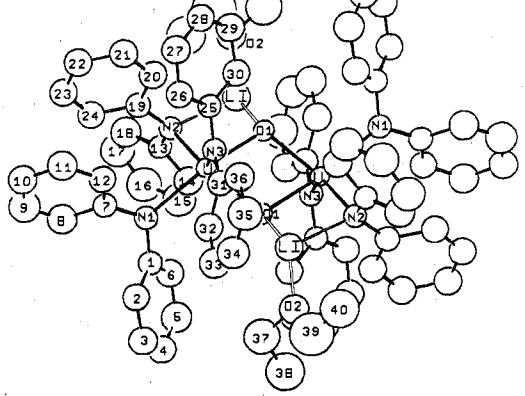

Figure 3. Molecular structure of $UO[(C_6H_5)_2N]_3LiO(C_2H_5)_2$ dimer.

$U(NEt_2)_4$[5] and $U_3(CH_3NCH_2CH_2NCH_3)_6$.[6] Both for N(1) and N(3) the three bonds are coplanar as is the rule for terminal amide groups. Atom N(2) is also coordinated to the lithium atom, and it is not coplanar with its uranium and carbon neighbors. This four-coordination explains the longer distance U–N(2) = 2.44 Å and the lack of planarity aided our discovery of lithium in this crystal. The lithium atom is also

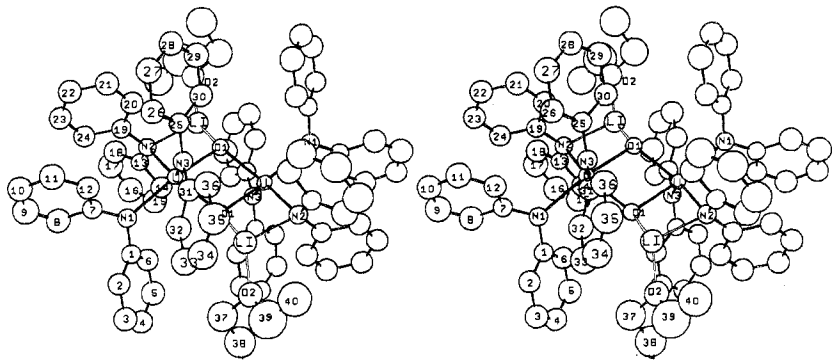

Figure 4. Stereogram of $UO[(C_6H_5)_2N]_3LiO(C_2H_5)_2$ dimer.

Table IV. Interatomic Distances (Å) in $U(dpa)_4$

U-N(1)	2.35 (2)	C(19)-C(20)	1.42 (3)
U-N(2)	2.27 (2)	C(19)-C(24)	1.42 (3)
U-N(3)	2.25 (2)	C(20)-C(21)	1.38 (3)
U-N(4)	2.21 (2)	C(21)-C(22)	1.39 (3)
N(1)-C(1)	1.50 (3)	C(22)-C(23)	1.40 (3)
N(1)-C(7)	1.38 (3)	C(23)-C(24)	1.35 (3)
N(2)-C(13)	1.41 (3)	C(25)-C(26)	1.42 (3)
N(2)-C(19)	1.40 (3)	C(25)-C(30)	1.37 (3)
N(3)-C(25)	1.40 (3)	C(26)-C(27)	1.38 (3)
N(3)-C(31)	1.37 (3)	C(27)-C(28)	1.40 (3)
N(4)-C(37)	1.48 (3)	C(28)-C(29)	1.34 (3)
N(4)-C(43)	1.42 (3)	C(29)-C(30)	1.40 (3)
C(1)-C(2)	1.42 (3)	C(31)-C(32)	1.39 (3)
C(1)-C(6)	1.38 (3)	C(31)-C(36)	1.42 (3)
C(2)-C(3)	1.41 (3)	C(32)-C(33)	1.41 (3)
C(3)-C(4)	1.35 (3)	C(33)-C(34)	1.32 (3)
C(4)-C(5)	1.40 (3)	C(34)-C(35)	1.37 (3)
C(5)-C(6)	1.36 (3)	C(35)-C(36)	1.36 (3)
C(7)-C(8)	1.40 (3)	C(37)-C(38)	1.36 (3)
C(7)-C(12)	1.37 (3)	C(37)-C(42)	1.39 (4)
C(8)-C(9)	1.41 (3)	C(38)-C(39)	1.38 (3)
C(9)-C(10)	1.36 (3)	C(39)-C(40)	1.35 (4)
C(10)-C(11)	1.35 (3)	C(40)-C(41)	1.37 (4)
C(11)-C(12)	1.42 (3)	C(41)-C(42)	1.37 (4)
C(13)-C(14)	1.41 (3)	C(43)-C(44)	1.36 (3)
C(13)-C(18)	1.43 (3)	C(43)-C(48)	1.39 (3)
C(14)-C(15)	1.39 (3)	C(44)-C(45)	1.36 (3)
C(15)-C(16)	1.33 (3)	C(45)-C(46)	1.41 (3)
C(16)-C(17)	1.35 (3)	C(46)-C(47)	1.39 (3)
C(17)-C(18)	1.41 (3)	C(47)-C(48)	1.35 (3)

Table V. Selected Angles (deg) in $U(dpa)_4$

N(1)-U-N(2)	139.2 (7)	U-N(2)-C(13)	136 (2)
N(1)-U-N(3)	100.8 (7)	U-N(2)-C(19)	105 (2)
N(1)-U-N(4)	96.3 (7)	C(13)-N(2)-C(19)	119 (2)
N(2)-U-N(3)	98.6 (7)	U-N(3)-C(25)	103 (2)
N(2)-U-N(4)	115.7 (7)	U-N(3)-C(31)	137 (2)
N(3)-U-N(4)	99.0 (7)	C(25)-N(3)-C(31)	120 (2)
U-N(1)-C(1)	95 (2)	U-N(4)-C(37)	101 (2)
U-N(1)-C(7)	142 (2)	U-N(4)-C(43)	137 (2)
C(1)-N(1)-C(7)	120 (2)	C(37)-N(4)-C(43)	119 (2)

coordinated to the bridging oxygen atom O(1) and to the ether oxygen O(2).

$U(dpa)_4$ was synthesized by both reactions 1 and 2. The driving force for the transamination reaction 1 is attributed to the lower pK_a of diphenylamine over diethylamine, although the exact pK_a values for the two amines are not known. Reaction 2 is a direct route to $U(dpa)_4$ and has been employed for many metal amides.[2,5,10,16-20] However, the thermal instability of $U(dpa)_4$ rules out sublimation as a method of purification, and successive recrystallizations from a solvent must be used. On the other hand, the $U(dpa)_4$ formed in reaction 1 crystallizes directly from the reaction mixture and needs no further purification (yield ~80%). However, the low yield of $U(NEt_2)_4$ from UCl_4 limits the overall utility of reaction 1.

Table VI. Interatomic Distances (Å) in $(UO(dpa)_3LiOEt_2)_2$

U-U	3.507 (1)	C(13)-C(14)	1.41 (2)
U-O(1)	2.16 (1)	C(13)-C(18)	1.37 (2)
U-O(1)′	2.20 (1)	C(14)-C(15)	1.38 (2)
U-N(1)	2.33 (1)	C(15)-C(16)	1.35 (2)
U-N(2)	2.44 (1)	C(16)-C(17)	1.35 (2)
U-N(3)	2.34 (1)	C(17)-C(18)	1.38 (2)
Li-O(1)	1.93 (3)	C(19)-C(20)	1.35 (2)
Li-O(2)	1.89 (3)	C(19)-C(24)	1.43 (2)
Li-N(2)	2.20 (3)	C(20)-C(21)	1.39 (2)
N(1)-C(1)	1.42 (2)	C(21)-C(22)	1.39 (2)
N(1)-C(7)	1.41 (2)	C(22)-C(23)	1.32 (2)
N(2)-C(13)	1.43 (2)	C(23)-C(24)	1.35 (2)
N(2)-C(19)	1.40 (2)	C(25)-C(26)	1.37 (2)
N(3)-C(25)	1.42 (2)	C(25)-C(30)	1.39 (2)
N(3)-C(31)	1.42 (2)	C(26)-C(27)	1.41 (2)
C(1)-C(2)	1.39 (2)	C(27)-C(28)	1.33 (2)
C(1)-C(6)	1.38 (2)	C(28)-C(29)	1.35 (2)
C(2)-C(3)	1.40 (2)	C(29)-C(30)	1.45 (2)
C(3)-C(4)	1.33 (2)	C(31)-C(32)	1.40 (2)
C(4)-C(5)	1.37 (2)	C(31)-C(36)	1.37 (2)
C(5)-C(6)	1.39 (2)	C(32)-C(33)	1.41 (2)
C(7)-C(8)	1.43 (2)	C(33)-C(34)	1.38 (2)
C(7)-C(12)	1.38 (2)	C(34)-C(35)	1.28 (2)
C(8)-C(9)	1.28 (2)	C(35)-C(36)	1.43 (2)
C(9)-C(10)	1.37 (2)	O(2)-C(37)	1.42 (2)
C(10)-C(11)	1.37 (2)	O(2)-C(39)	1.40 (2)
C(11)-C(12)	1.36 (2)	C(37)-C(38)	1.54 (3)
		C(39)-C(40)	1.44 (3)

Table VII. Selected Angles (deg) in $(UO(dpa)_3LiOEt_2O)_2$

N(1)-U-N(2)	91.6 (3)	U-N(1)-C(1)	123 (1)
N(1)-U-N(3)	100.3 (3)	U-N(1)-C(7)	121 (1)
N(1)-U-O(1)	100.1 (3)	C(1)-N(1)-C(7)	116 (1)
N(1)-U-O(1)′	160.9 (3)	U-N(2)-C(13)	126 (1)
N(2)-U-N(3)	132.6 (3)	U-N(2)-C(19)	96 (1)
N(2)-U-O(1)	127.1 (3)	U-N(2)-Li	87 (1)
N(2)-U-O(1)′	79.6 (3)	C(13)-N(2)-C(19)	122 (1)
N(3)-U-O(1)	96.0 (3)	C(13)-N(2)-Li	102 (1)
N(3)-U-O(1)′	98.1 (3)	C(19)-N(2)-Li	119 (1)
O(1)-U-O(1)′	72.9 (3)	U-N(3)-C(25)	123 (1)
U-O(1)-U	107.1 (3)	U-N(3)-C(31)	122 (1)
U-O(1)-Li	128.4 (8)	C(25)-N(3)-C(31)	115 (1)
U′-O(1)-Li	101.5 (8)	C(37)-O(2)-C(39)	105 (2)
O(1)-Li-N(2)	92 (1)	C(37)-O(2)-Li	118 (2)
O(1)-Li-O(2)	130 (2)	C(39)-O(2)-Li	132 (2)
N(2)-Li-O(2)	112 (2)		

The dark, intense, blood red color $U(dpa)_4$ is probably due to the involvement of the aromatic rings of the amide group in ligand to metal charge-transfer transitions. These charge-transfer transitions can be followed throughout the course of reaction 1, suggesting the formation of intermediates during the exchange. The original green solution of $U(NEt_2)_4$ slowly changes from yellow to red in a period of approximately 6 h. This color change suggests the diethylamide groups are slowly exchanged with diphenylamide groups, shifting the visible transitions to longer wavelengths with the replacement of each diethylamide.

Table VIII. Proton Magnetic Resonance Spectra of $U[N(C_6H_5)_2]_4$ in Toluene-d_8 and THF-d_8 (All Shifts Are Relative to TMS)[a]

Solvent	Ortho	Meta	Para	Temp, °C
Toluene-d_8	+3.8 (d)[b]	+6.8 (t)[b]	+4.45 (5)	110
	+4.0 (d)	+6.3 (5)	+3.5 (5)	14
	+ (broad doublet)	+6.7	+5.4 (broad singlet)	−75
THF-d_8	−6.4 (d)	+2.7 (5)	+1.2 (5)	25

[a] + indicates downfield from TMS; − indicates upfield from TMS. [b] d = doublet, t = triplet.

Figure 5 shows the proton magnetic spectrum of $U(dpa)_4$ in toluene-d_8 at various temperatures.[20] Table VIII lists the relative shifts with respect to TMS. From 110 to −50 °C the peaks exhibit a linear temperature-dependent paramagnetic effect. If we assume that all four nitrogens are tetrahedrally equivalent in solution then the paramagnetic shifts are due to a Fermi contact hyperfine interaction because the pseudocontact term would vanish with tetrahedral symmetry.[21] At a temperature of ca. −50 °C the upfield peak disappears and the two downfield peaks coalesce into one broad peak. As the temperature is lowered further, only two broad peaks can be found. These observations suggest that some type of exchange is taking place below −50 °C and we are unable to resolve the spectrum of the molecular species. The large upfield shifts observed in the THF-d_8 spectra suggest a change in symmetry apparently due to pseudocontact shifts. This effect has been seen in other uranium amides,[4,5] where the ether solvents appear to coordinate to the metal. The ^1H NMR of the uranium amides are being explored further.

Figure 6 shows the optical and near-IR spectra in benzene and diethyl ether. Table IX lists the extinction coefficients of $U(dpa)_4$ and compares them with $U(NEt_2)_4$.[4] The spectral similarities of the two compounds suggest the ligand has little effect on the nature of the f → f transitions. As in $U(NEt_2)_4$, the differences between the benzene and ether spectra are attributed to the complexing ability of the solvents.[4]

The inverse molar magnetic susceptibility of $U(dpa)_4$ in the temperature range 4.2–100 K is shown in Figure 5. At low temperatures ($T < 20$ K) the susceptibility becomes temperature independent while above 30 K the susceptibility follows the Curie–Weiss law with

$$\chi_M = C_M/(T + \Theta)$$

and $C_M = 1.00$, $\mu_{eff} = 2.84 \pm .06\ \mu_B$, and $\Theta = 24.8$ K.

A plausible interpretation of the magnetic susceptibility data can be based on the ordering of the crystal field states by the distorted tetrahedral crystal field. Under T_d symmetry, a $J = 4$ state is decomposed into a singlet (Γ_1), a doublet (Γ_3), and two triplets (Γ_4 and Γ_5). If we assume the point charge model gives at least the correct signs for the crystal field parameters, then the lowest crystal field state would be either a Γ_5 or a Γ_1 state.[22] Assuming L–S coupling, g_J is equal to $^4/_5$ for the $^3H_4$ state of U^{4+}, and the effective magnetic moment for the Γ_5 state is $\mu_{eff} = 2.828\ \mu_B$[23] in excellent agreement with the observed $\mu_{eff} = 2.84 \pm .06\ \mu_B$ above approximately 40 K. Because of the distorted tetrahedral crystal field the Γ_5 state can be split into three singlets or a singlet and a doublet. These splittings of the order of ~25 cm^{-1} could result in the observed temperature-independent susceptibility below 30 K.

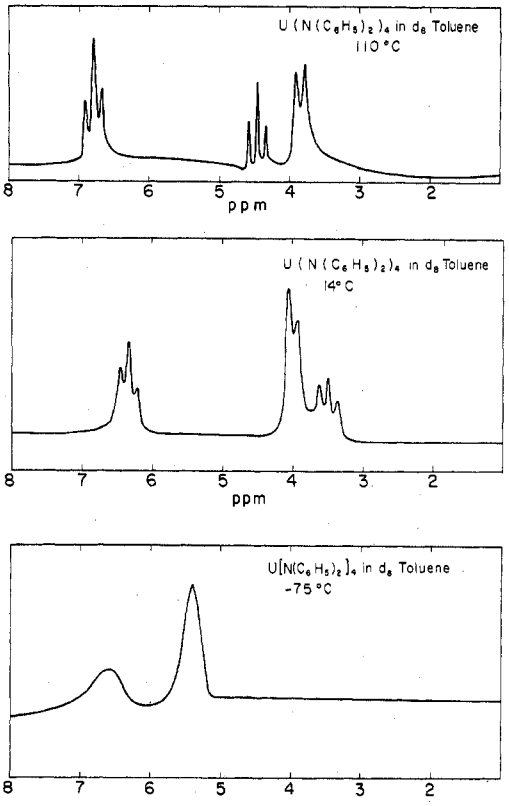

Figure 5. Proton magnetic resonance spectra of $U[N(C_6H_5)_2]_4$ in toluene-d_8 at various temperatures.

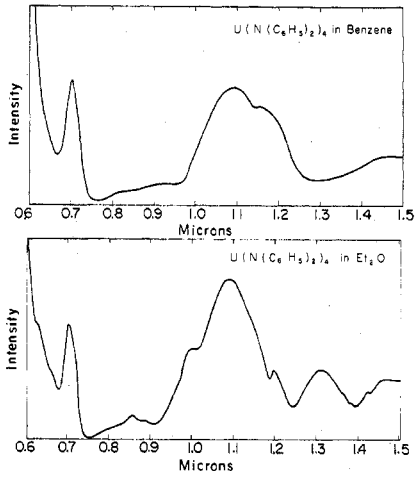

Figure 6. Optical spectra of $U[N(C_6H_5)_2]_4$ in benzene and diethyl ether.

The oxo-bridged complex was formed from the filtrate of reaction 2 by seepage of air through the ground glass joints. The diethyl ether solvent attacks the silicone grease allowing air to diffuse into the flask. The reagents of this reaction are uncertain, but the results are reproducible. Air has been established as an essential reagent, while the Li(dpa) appears to be a limiting reagent. Further addition of air produces black

Table IX. Peak Positions (λ in μm) and Extinction Coefficients of $U(dpa)_4$ and $U(NEt_2)_4$ in Various Solvents

	1		2		3		4		5	
Species	λ	ϵ	λ	ϵ	λ	ϵ	λ	ϵ	λ	ϵ
$U(dpa)_4$ in benzene	0.709	46	1.099	43	1.160	35				
$U(NEt_2)_4$ in benzene	0.692	47	1.090	27	1.172	26				
$U(dpa)_4$ in Et_2O	0.710		1.005		1.096		1.192		1.307	
$U(NEt_2)_4$ in Et_2O	0.638	28	.990	20	1.070	32			1.302	19

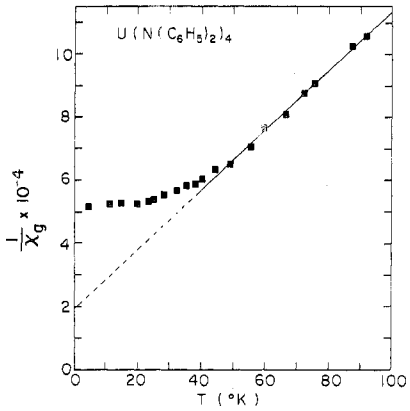

Figure 7. Inverse molar magnetic susceptibility of $U[N(C_6H_5)_2]_4$.

microcrystals, but no structure determination of these was possible.

We have found that uranium amides have a greater tendency to oligomerize than the d transition series amides. By proper choice of a bulky ligand we have been able to synthesize a monomer $U(N(C_6H_5)_2)_4$ in the solid state. The steric congestion is relieved in the oxygen-bridged product where one diphenylamide group is replaced, and the solid state structure is dimeric. In solution, $U(N(C_6H_5)_2)_4$ exhibits strong similarities to the other uranium amides. Once again the proton magnetic resonance and optical spectra indicate complexing with donating type solvents. In noncomplexing solvents, the tetrahedral structure is retained. It appears that with most of the uranium amides, the solid state structure is not necessarily the same as the solution species.

Acknowledgment. This work was done with support from the U.S. Energy Research and Development Administration.

Registry No. $U(dpa)_4$, 61900-16-1; $(UO(dpa)_3LiOEt_2)_2$, 62005-87-2; $U(NEt_2)_4$, 40678-59-9.

Supplementary Material Available: Formulas used in data reduction and listings of the structure factors (35 pages). Ordering information is given in any current masthead page.

References and Notes

(1) R. G. Jones, G. Karmas, G. A. Martin, Jr., and H. Gilman, *J. Am. Chem. Soc.*, **78**, 4285 (1956).
(2) K. W. Bagnall and E. Yanir, *J. Inorg. Nucl. Chem.*, **36**, 777 (1974).
(3) J. D. Jamerson and J. Takats, *J. Organomet. Chem.*, **78**, C23 (1974).
(4) J. G. Reynolds, A. Zalkin, D. H. Templeton, N. Edelstein, and L. K Templeton, *Inorg. Chem.*, **15**, 2498 (1976).
(5) J. G. Reynolds, A. Zalkin, D. H. Templeton, and N. M. Edelstein, *Inorg. Chem.*, **16**, 599 (1977).
(6) Professor J. Takats of University of Alberta, Alberta, Canada has informed us that he has also synthesized this compound and has characterized it by its proton magnetic resonance spectrum and mass spectrum.
(7) H. St. Räde, *J. Phys. Chem.*, **77**, 424 (1973).
(8) M. H. Chisholm, F. A. Cotton, M. Extine, and B. R. Stults, *J. Am. Chem. Soc.*, **98**, 4477 (1976).
(9) D. C. Bradley, M. B. Hursthouse, and C. W. Ewing, *Chem. Commun.*, 411 (1971).
(10) C. Heath and M. B. Hursthouse, *Chem. Commun.*, 143 (1971).
(11) D. C. Bradley, M. H. Chisholm, C. E. Heath, and M. B. Hursthouse, *Chem. Commun.*, 1261 (1969).
(12) F. A. Cotton, B. R. Stults, J. M. Troup, M. H. Chisholm, and M. Extine, *J. Am. Chem. Soc.*, **97**, 1242 (1975).
(13) M. H. Chisholm and W. Ruchert, *J. Am. Chem. Soc.*, **96**, 1249 (1974).
(14) O. Kennard, "International Tables for X-ray Crystallography", Vol. III, Kynoch Press, Birmingham, England, 1962, Table 4.2.4.
(15) D. C. Bradley, *MTP Int. Rev. Sci.: Inorg. Chem., Ser. One*, **5**, 82 (1972).
(16) D. C. Bradley and M. H. Chisholm, *Acc. Chem. Res.*, **9**, 272 (1976).
(17) D. C. Bradley and I. M. Thomas, *J. Chem. Soc.*, 3857 (1960).
(18) D. C. Bradley and I. M. Thomas, *Can. J. Chem.*, **40**, 449 (1962).
(19) D. C. Bradley and I. M. Thomas, *Can. J. Chem.*, **40**, 1355 (1962).
(20) The ^1H NMR results of Professor Takats are in good agreement with our work.
(21) D. R. Eaton and W. D. Phillips, *Adv. Magn. Reson.*, **1**, 103 (1965).
(22) K. R. Lea, J. J. M. Leash, and W. P. Wolf, *J. Phys. Chem. Solids*, **23**, 1381 (1962).
(23) C. A. Hutchison, Jr., and G. A. Candela, *J. Chem. Phys.*, **27**, 707 (1957).

Contribution from the Department of the Geophysical Sciences, The University of Chicago, Chicago, Illinois 60637

Mitridatite, $Ca_6(H_2O)_6[Fe^{III}_9O_6(PO_4)_9]\cdot 3H_2O$. A Noteworthy Octahedral Sheet Structure

PAUL BRIAN MOORE* and TAKAHARU ARAKI

Received November 23, 1976 AIC608439

A natural single crystal of mitridatite, asymmetric unit $Ca_6(H_2O)_6[Fe^{III}_9O_6(PO_4)_9]\cdot 3H_2O$, was studied in detail by three-dimensional x-ray diffractometry. The compound is monoclinic and possesses space group Aa, $Z = 4$, $a = 17.553$ (2), $b = 19.354$ (3), $c = 11.248$ (2) Å, $\beta = 95.84$ (1)°. $R = 0.068$ ($R_w = 0.082$) for 5547 independent reflections. X-ray diffraction data to $(\sin\theta)/\lambda = 0.70$ (Mo $K\alpha_1$ radiation) were collected on a Picker FACS-1 automated diffractometer and the structure was solved by Patterson, Fourier, chemical-intuitive and least-squares refinement techniques. The underlying principle is a compact sheet of composition $[Fe^{III}_9O_6(PO_4)_9]^{12-}$ oriented parallel to the {100} plane and located at $x \sim {}^1/_4$ and ${}^3/_4$. It has trigonal pseudosymmetry $a = 11.25$ Å (=c of mitridatite cell) and two-sided plane group $p31m$ and is locally isomorphic to a sheet of composition $[Na_9F_6(SO_4)_9]^{15-}$ found in the crystal structure of schairerite, $Na_{21}F_6Cl(SO_4)_7$, $Z = 3$. The sheet is built of octahedral Fe^{3+}–O edge-sharing nonamers decorated above, below, and in the plane by the PO_4 tetrahedra.

Introduction

Mitridatite, a basic calcium ferric phosphate, is a widely distributed although ill-defined phase in low-temperature sedimentary environments. Earlier described as crusts and nodules from the oolitic sedimentary iron ore deposits in the Kerch and Taman peninsulas, southern Russia,[1-3] it also occurs as a common product of weathering of exposed primary iron phosphates in pegmatites and other granitic rocks,[4] and in ferruginous soils, marls, and sandstones which have been impregnated with organic remains. Such field evidence suggests that the phase is quite stable and possibly one of the most important ferric phosphates formed under rather neutral conditions and ambient temperatures as prevail on the surface of the Earth. Its typical appearance as dull-green to brownish-green earthy stains and films are hardly good distinguishing characters and only the trained eye lifts it out of its undeserved obscurity in natural systems.

Mitridatite has posed some difficult problems for the investigator. Satisfactory single crystals are a great rarity and variable composition of cryptocrystalline masses is typical. The